A new magnetic graphitized carbon black TiO_2 composite for phosphopeptide selective enrichment in shotgun phosphoproteomics.

Susy Piovesana[1], Anna Laura Capriotti[1], Chiara Cavaliere[1], Francesca Ferraris[1], Daniel Iglesias[2], Silvia Marchesan[2], Aldo Laganà[1]

1. Dipartimento di Chimica, Sapienza Università di Roma, Piazzale Aldo Moro 5, 00185 Rome, Italy

2. Dipartimento di Scienze Chimiche e Farmaceutiche, Università di Trieste, Via L. Giorgieri 1, 34127 Trieste, Italy

ABSTRACT: Graphitized carbon black (GCB) has been employed for extraction of several classes of analytes, due to the large surface area and the unique chemistry of its surface groups that allows to extract a wide range of analytes, including polar, acidic compounds. Despite the fact that structurally-related materials, such as graphene, found application as hybrid-components in phosphoproteomics, surprisingly, GCB has never been used for the selective enrichment of phosphopeptides. For this purpose, in the present work we used GCB to prepare a magnetic composite with TiO_2 (mGCB@TiO_2) that was then applied to yeast total extracts. We exploited the high surface area provided by nanostructures, the presence of nano-TiO_2 for selective binding of phosphopeptides, and the magnetic responsiveness of magnetite for solid-phase separation. The material was extensively characterized at each modification step by transmission electron microscopy, Fourier-transformed infrared spectroscopy, thermogravimetric analysis, Raman spectroscopy and porosimetry. Next, the new system was applied for the enrichment of casein phosphopeptides from a simulated tryptic digest with bovine serum albumin (BSA:casein, 100:1). Finally, after assessing the potential applicability, the composite was employed for enriching phosphopeptides from yeast protein digests. This allowed us not only to optimize the enrichment protocol, but also to fully compare its performance to commercial TiO_2 spin columns. To achieve this aim, the optimized enrichment protocol was included in a typical shotgun proteomics analytical workflow based on nanoHPLC-MS/MS analysis.

INTRODUCTION

Protein phosphorylation is a dynamic and reversible post-translational modification that is widely used in biological systems to regulate protein-protein interactions and thus, to rapidly activate or deactivate signaling pathways. It has proven to play a key role in several biological processes, such as the cellular signaling and communication,[1] cell adhesion and migration,[2] transcriptional and translational regulation,[3] cell division and apoptosis.[4] Gaining knowledge about these pathways is strongly related to cell activity and it may help shedding light on relevant physiological and pathological conditions.[5] In this sense, proteomics technologies and mass spectrometry have become the leading tools for the analytical chemist interested in the study of transient post-translational modifications. However, despite the great potential of HPLC-MS/MS in the field, direct analysis is generally not possible without prior enrichment of target proteins or peptides. This is due to a number of factors that, especially in the case of phosphorylations, can be ascribed to 1) sub-stoichiometric extent of phosphorylated proteins, 2) poor ionization efficiency, and 3) signal suppression by the abundant non-phosphorylated peptides. As a result, highly selective enrichment strategies for phosphorylated proteins or peptides prior to HPLC-MS/MS analysis have become mandatory for efficient detection.[6] To this end, several approaches were described in the literature, such as: immobilized metal ion affinity chromatography (IMAC), metal oxide affinity chromatography (MOAC), inorganic salt affinity chromatography with lanthanide ions, co-precipitation, ion exchange chromatography, chemical derivatization, and immunoprecipitation.[7] Amongst the various methods, affinity chromatography is the most widely used. Typically, the affinity of phosphate moieties to a metal ion is exploited to selectively capture phosphopeptides or phosphoproteins from a more complex mixture, thus allowing their enrichment and further processing. Popular metal ions used in IMAC include Fe^{3+},[6] Ga^{3+},[8] Ti^{4+} [9] and Zr^{4+}.[10] As for MOAC, popular metal oxides are TiO_2[11] and ZrO_2.[12] Such materials can be used in analytical column-, miniaturized column-, or batch-format. Taken individually, IMAC and MOAC do not usually provide a comprehensive pro-

file of the phosphoproteome, due to analyte physico-chemical diverse features. To overcome this limitation, combined strategies have been developed[13] to enrich multi-phosphorylated peptides by IMAC and mono-phosphorylated peptides by MOAC. Alternatively, protocols were improved for existing systems, as in the case of the recently described HILIC-mode for TiO_2[14] and Fe^{3+}-IMAC column separation.[15]

In this context, the development of new stationary phases for use in phosphoproteomics is of great demand to fill the existing gaps and to allow for a comprehensive analysis. Popular methods for phosphopeptide enrichment consist of stationary phases in batch format, and self-made or commercial micro-columns packed into pipette tips.[15] Some advantages over miniaturized column format can be found by using solid-phase magnetic separation. With respect to packed micro-columns, the use of magnetic phases avoids the step of column packing. Besides, the large surface area and facile dispersibility of micro-beads or nanomaterials in the bulk solvent provides increased contact with the target analytes, thus favoring their enrichment. Finally, magnetic phases can be easily recovered by applying an external magnetic field, and this facilitates the removal of unbound species in the loading and washing steps, while allowing the enrichment of bound species.[16]

In the present study, a nanostructured composite was prepared using for the first time graphitized carbon black (GCB) as a support for phosphopeptide enrichment. This is surprising considering that structurally-related graphene has found similar applications to support TiO_2;[17,18] also in magnetic materials.[19] However, it is worth noting that graphene technology is still under development and it comprehends very diverse materials in terms of physico-chemical properties and purity, with batch-to-batch differences that at times can be significant. In addition, depending on the manufacturer and production method, contamination by other components, such as surfactants, is an important aspect that should not be neglected. By contrast, GCB is a well-characterized component of commercial products that has been available on the market already for several years. Its use as adsorbent in gas and liquid chromatography is well-established, as it non-specifically concentrates a wide variety of organic analytes mainly through London forces. It can be found both in the porous or non-porous form, and it could potentially be a suitable support for composite production due to its unique features. In fact, we chose non-porous GCB as it allows for rapid processing since analyte adsorption does not require dispersion into solid phase pores. Yet, non-porous GCB displays a large surface area (100 $m^2\ g^{-1}$) and has the capacity to interact also with polar molecules, especially acidic compounds.[20,21] These properties are very interesting, and even more so, if coupled to convenient magnetic solid-phase extraction for the enrichment of target peptides and to the selectivity for phosphopeptides by TiO_2. The nanostructured material was prepared and extensively characterized at each modification step by different techniques. Preliminary experiments were performed with a simplified peptide mixture of standard proteins, to assess the potential of the system for analytical use. This approach, together with application on a real sample of small complexity is the standard approach in method development for new materials, and several examples can be found in the literature.[22] In most cases, MALDI MS is employed for enrichment testing, however such an approach is limited by many factors. First, final real-world applications are for analyte enrichment from very complex samples, such as tissue and cell extracts. Such samples need more high-throughput and comprehensive techniques for appropriate analysis, thus shotgun proteomics workflows based on HPLC separation coupled to tandem high resolution MS is needed. In this regard, only a few examples are described in the literature where tests were extended from the proof-of-concept stage to application to complex samples.[23–28] Second, analysis of complex samples by shotgun proteomics is mandatory for a relevant comparison amongst analytical methods, in order to point out key differences and identify method scope. Thus, in the present study the new mGCB@TiO_2 composite was first tested on a mixture of two standard protein digests, then applied to the enrichment of phosphopeptide from yeast total protein extracts and results assessed by nanoHPLC-MS/MS. After the optimization of the enrichment protocol, the system was compared against a commercial TiO_2 spin column kit.

■ EXPERIMENTAL SECTION

Reagents and Materials.

All chemicals, reagents, protein standards and organic solvents of the highest grade available were provided by Sigma-Aldrich (St. Luis, MO, USA) unless otherwise stated. Trypsin and Trypsin/Lys-C Mix, Mass Spec Grade, were provided by Promega (Madison, WI, USA). Doubled distilled water (ddH2O) was prepared by an arium 611 VF system from Sartorius (Göttingen, Germany).

Instruments.

Transmission electron microscopy (TEM) images were obtained with a Philips EM 208 transmission electron microscope with a 100 keV acceleration voltage and standard loop filament, Olimpus Morada 2K x 2K CCD camera. The calibration is accurate to ± 5%. A drop of a concentrated dispersion of the corresponding material in methanol was dropcasted on top of the grid (carbon film, 300 mesh, copper). then, the solvent was evaporated under vacuum before the analysis.

Thermogravimetric analysis (TGA) was performed on TA Instruments TGA Q500 under an air flow of 90 ml min^{-1} with a ramp of 10 °C/min from 100 to 800 °C. Analyses were run in duplicates.

Fourier transform infrared spectroscopy (FT-IR) spectra were recorded on PerkinElmer 2000 spectrophotometer. Sample pellets were prepared using anhydrous KBr and the corresponding material. The transmittance of the pellets was measured from 4000 cm^{-1} to 400 cm^{-1}.

Raman spectra were recorded on a Renishaw instrument, model Invia reflex equipped with 532 laser operating at 22.5 W. After acquisition, the spectra were normalized with respect to the G band and then the maximum intensity ratio of the D and G band were calculated. Different points along the samples were taken and averaged out to confirm the homogeneity of the samples.

Porosimetry analysis was performed on 3Flex Surface Characterization Analyzer (Micromeritics Instrument Corporation, Norcross, GA, U.S.A.).

Synthesis of magnetic-graphitized carbon black TiO_2 hybrid material.

The mGCB@TiO_2 composite was prepared based on a previous report for carbon nanotubes with some modification.[29] GCB (Supelclean ENVI-Carb, Sigma-Aldrich, St. Louis, MO) was first activated by treating 400 mg with 50 mL concentrated nitric acid, under stirring at room temperature for 7 h. Afterwards, the material was extensively washed with water until neutral pH and dried overnight at 50 °C. The just described oxidation with nitric acid was skipped for non-oxidized GCB material. GCB, either oxidized or non-oxidized (150 mg), was then magnetized treating with $FeCl_3 \cdot 6H_2O$ (810 mg) trisodium citrate (150 mg), sodium acetate (3.6 g), and poly(ethylene glycol)-10k (1.0 g) in 40 mL of ethylene glycol solution. The mixture was sonicated for 3 h and then sealed in a 125 mL autoclave for 10 h at 200 °C. When cold, the autoclave was opened and the product washed with water and ethanol. Finally, 30 mg of the magnetic graphitized carbon black (mGCB) was sonicated in 50 mL isopropyl alcohol for 30 min and added with 20 µL diethylamine. After stirring for 5 min, the mixture was added with 1.5 mL of titanium isopropoxide, transferred into the autoclave and kept at 200 °C for 24 h. The final product was washed with water and ethanol, dried and finally calcined at 400 °C for 2 h.

Proteomic sample preparation.

Bovine serum albumin (BSA) and casein tryptic digests were prepared as described previously.[28] Yeast protein extracts were prepared by the freezing and grinding method. Briefly, 1 g of commercial yeast paste purchased in a local supermarket was ground to fine powder with mortar and pestle with the aid of liquid nitrogen to lyse yeast cells. Then, 400 mg of the powder were added with 13.4 mL of cold lysis buffer (8 mol L^{-1} urea in 50 mmol L^{-1} Tris-HCl, pH 8, added with MSSAFE protease and inhibitor cocktail (Sigma-Aldrich, St. Louis, MO), used according to manufacturer's instructions. The sample was vortexed for 10 min, then centrifuged at 9400 x g at 4 °C for 10 min to sediment cell debris, and finally transferred into a new tube. Protein concentration was determined by the Bradford assay. For digestion, 900 µg protein aliquots were diluted to 1 µg μL^{-1} with 8 M urea in Tris-HCl buffer, then treated with 200 mmol L^{-1} dithiothreitol (DTT) in Tris-HCl buffer and 200 mmol L^{-1} iodoacetamide (IAA) in Tris-HCl as described for BSA and casein samples. Digestion was performed with Trypsin/Lys-C Mix (enzyme to protein ration, 1:25), allowing Lys-C digestion for 4 h at 37 °C and then diluting the urea concentration to 1 mol L^{-1} for tryptic overnight digestion. Digestion was terminated with trifluoroacetic acid (TFA) and then samples were desalted, and dried down as described for BSA and casein.

Selective Enrichment of Phosphopeptides.

For each enrichment experiment, a suitable amount of mGCB@TiO_2 was weighed, then conditioned with 100 µL of washing buffer (ACN:H_2O, 80:20 with 0.4% TFA) slightly agitating the suspension for 2 min. After 1 min centrifugation (2300 x g) to sediment the entire solution, the magnetic phase was recovered and the supernatant discarded; then the phase was conditioned with the loading buffer (28% lactic acid, 57% ACN, 14% H_2O, 0.2% TFA) as before. After this step, samples reconstituted with the loading buffer (2 µg μL^{-1} concentration) were added and mildly shaken for 30 min to allow binding. After centrifugation and magnetic recovery of the loaded mGCB@TiO_2, the supernatant was discarded and the phase washed once with the loading buffer and twice with the washing buffer (100 µL each, 2 min shaking). A four-step elution was performed, twice with 100 µL of elution buffer 1 (1.5% NH_3 (aq)) and twice with 100 µL of elution buffer 2 (5% pyrrolidine (aq)), each time gently shaking for 5 min. Combined eluates were acidified with 2.5% TFA to pH 2.5, desalted, dried down in a Speed-Vac SC250 Express (Thermo Savant, Holbrook, NY, USA) and resuspended with 100 µL 0.1% formic acid (FA). Samples were stored at -80 °C until analysis. For each tested condition, two experimental replicates were performed. For comparison purposes, enrichment was performed on commercial Pierce™ TiO_2 Phosphopeptide Enrichment and Clean-up Kit (ThermoFisher Scientific) according to instruction manual.

NanoHPLC-MS/MS analysis and peptide identification.

Twenty uL peptide mixtures were separated by RP chromatography using the Dionex Ultimate 3000 (Dionex Corporation Sunnyvale, CA, USA). Samples were on-line preconcentrated on a µ-precolumn (Dionex, 300 µm i.d. × 5 mm Acclaim PepMap 100 C18, 5 µm particle size, 100 Å pore size), employing a premixed mobile phase ddH_2O:ACN 98:2 (v/v) containing 0.1% (v/v) TFA at a flow-rate of 10 µL min^{-1}.

BSA:casein mixtures were separated as described in our previous work,[28] but employing a Dionex Ultimate 3000 (Dionex Corporation Sunnyvale, CA, USA) coupled to a LTQ Orbitrap XL (Thermo Scientific, Bremen, Germany) mass spectrometer.

Yeast samples were separated on an EASY-Spray column (Thermo Scientific, Bremen, Germany) operated at 200 nL min^{-1} and at 40 °C. A 280 min long multi-step gradient was employed to separate peptides, using ddH_2O with 0.1% FA as phase A and ACN with 0.1% FA as phase B. Starting from 1% phase B, such composition was maintained for 5 min, then phase B was linearly increased to 5% within 2 min; afterwards, phase B was first increased to 30% within 187 min, then to 50% within the following 13 min and 80% in 5 min. Phase B was maintained at 80% for 20 min to rinse the column and finally lowered to 1% within 1 min. The column was then equilibrated at this percentage for 44 min. Full scan and MS/MS analysis of eluting peptides were performed by a Orbitrap Elite hybrid ion trap-Orbitrap mass spectrometer (Thermo Scientific, Bremen, Germany) in the m/z range of 400-1800 Da and 60,000 (Full Width Half Maximum at m/z 400) resolution for the full scan. A data dependent mode acquisition was enabled, in top 20 mode, rejecting +1 and unassigned charge states, using a normalized collision energy of 35%, and an isolation window of 2 m/z. Ion trap and Orbitrap maximum ion injection times were set to 100 and 200 ms, respectively. Automatic gain control was used to prevent overfilling of the ion traps and was set to 1×10^6 for full FTMS scan, and 1×10^4 ions in MS n mode for the linear ion trap. To minimize redundant spectral acquisitions, dynamic exclusion was enabled with a repeat count of 1 and a repeat duration of 30 s with exclusion duration of 70 s. For each sample, three technical replicates were performed.

Database search and peptide identification.

Peptide identification for the acquired raw MS/MS data files from Xcalibur software (version 2.2 SP1.48, Thermo Fisher Scientific) was performed searching Uniprot database with Proteome Discoverer software (version 1.3, Thermo Scientific) and the Mascot (v.2.3.2, Matrix Science) search engine, as previously described,[28] using the *Bos taurus* taxonomy (5986 entries) for BSA and casein samples, and the *S. cerevisae* taxonomy (7803 entries) for yeast samples.

■ RESULTS AND DISCUSSION

Characterization of the mGCB@TiO_2 material.

The nanostructured materials were thoroughly characterized at each modification step to assess morphological and structural changes. TGA was performed in air to quantify the increase of inorganic material during the last two stages of composite formation (Figure 1a). High purity of pristine GCB was confirmed by the absence of weight loss both at low temperatures (indicative of absence of amorphous carbon and organic contaminants) and at temperatures above 720 °C (indicative of absence of inorganic impurities). Besides, the sharp weight loss in the 650-720 °C range confirmed high homogeneity for the graphitic structure of GCB.

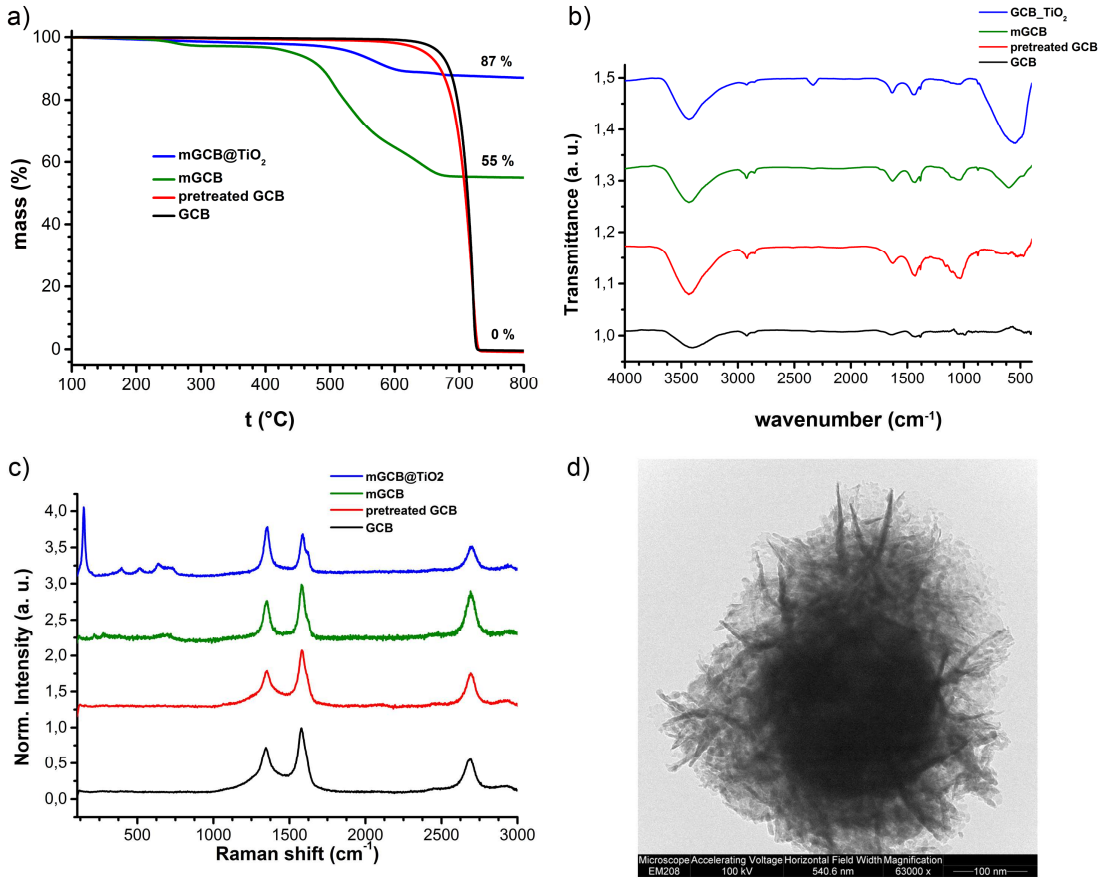

Figure 1. a) TGA curves, b) FT-IR spectra, c) Raman spectra for mGCB@TiO_2 final and intermediate materials and d) TEM image of the final product.

Graphitic materials are typically robust towards harsh chemical environments, and this behavior was evident as the oxidized GCB maintained a TGA profile similar to the pristine material, with only a 2% weight loss at 600 °C as a result of the chemical oxidation. As expected, more dramatic changes were registered for the subsequent steps of composite assembly, with the inorganic components increasing first to 55% after magnetization, and then to a remarkable 87% after *in situ* growth of TiO_2.

FT-IR analysis was also performed to monitor modifications in the chemical structure of the materials (Figure 1b). Also in this case, GCB displayed a spectrum indicative of high quality, as just minor features were observed, including the typical C-H stretchings at 2880 cm^{-1} and 2865 cm^{-1}, and a weak signal for C-H rocking at 1350 cm^{-1} and for C-H scissoring at 1430 cm^{-1}. After treatment with nitric acid, a broad signal for the O-H stretch dominated the spectrum in the region 3000-3600 cm^{-1}, while signals in the regions 1400-1700 cm^{-1} and 1000-1300 cm^{-1} were compatible with the presence of C=O and C-O bonds. Importantly, after magnetization, the indicative peaks for magnetite nanoparticles were observed below 600 cm^{-1}, including the characteristic peak at 590 cm^{-1} for the Fe-O bond, and the minor shoulder at 470 cm^{-1}.[30] Finally, after the last step of composite preparation, presence of TiO_2 was evident from the strong signal centered in the region 500-600 cm^{-1}.[31]

Raman analysis revealed presence of the typical D, G, and 2D bands at ca. 1350, 1580 and 2700 cm^{-1} respectively, as expected for GCB, with an I_D/I_G of 0.72. I_D/I_G ratios did not change significantly after acid treatment, confirming once again overall preservation of GCB structure, with mild oxidation as suggested by TGA and FT-IR analysis. Presence of magnetite was next confirmed by the signal at ca. 670 cm^{-1}. After growth of TiO_2, signals appearance at 147, 198, 396, 516, and 639 cm^{-1} were compatible with the typical profile of the five active modes of anatase structure. Overall, Raman analysis was in agreement with the other spectroscopic data discussed above. Importantly, it confirmed the achievement of each GCB modification step, and successful preparation of the composite material.

TEM analysis was also performed to monitor morphological changes at each step of composite preparation (Figure 1d, Supporting Information S1). Also this technique confirmed the high homogeneity and purity of GCB graphitic structure, which was pre-

served after oxidation. Magnetization resulted in the appearance of spherical nanoparticles (100-300 nm in diameter) bound to the surface of GCB, and displaying the high contrast that is typical for inorganic components. *In situ* growth of TiO_2 resulted in the complete surface coverage of magnetized GCB, as only high contrast clusters of nanoparticles were observed, with a characteristic nanomorphology.

The porosimetry analysis was performed at all stages of mGCB@TiO_2 preparation (Supporting Information S1). The starting GCB provided a surface area of 98.0 ± 1 m^2 g^{-1}, as declared by the manufacturer. The pore investigation provided a total pore volume of 0.60 cm^3 g^{-1}, with a mesopore structure and diameters in the range 20-35 Å and 80-800 Å (largest population, maximum at 460 Å). The magnetization process reduced the available surface area to 55.0 ± 0.5 m^2 g^{-1} and the pore volume as well, to 0.30 cm^3 g^{-1}. The structure was still mesoporous with no significant changes in pore diameters (20-40 Å and 80-800 Å) but different distribution, since the first group was representative of half the population. Finally, such trend was more evident in the final product, were the surface area was further reduced to 22.6 ± 0.5 m^2 g^{-1}, and the pore volume to 0.30 cm^3 g^{-1}. The number of mesopores was also reduced, in the ranges 20-40 Å and 50-500 Å.

Preliminary experiments on the simulated complex peptide mixture.

To demonstrate the selectivity of the mGCB@TiO_2 composite, the enrichment from a moderately complicated sample, made up of standard phosphoprotein (bovine β-casein) tryptic digest mixed to BSA tryptic digest in a 1:100 ratio, was first used to evaluate the performance of this new material. This type of sample was chosen because it is usually employed to test the enrichment efficiency of new phosphopeptide enrichment phases, due to possibility of simulating conditions of complex samples.[32] In fact, casein, which is the precursor protein of phosphopeptide, is used at low concentration to mimic the low abundance of phosphopeptide in real samples, whereas BSA is employed to complicate the peptide mixture with non-modified peptides. For these preliminary studies two experimental replicates were performed and 300 µg tryptic digest was loaded on 5 mg mGCB@TiO_2 stationary phase. For the selected simplified system, the performance was good, and the results for the two experimental replicates are reported in Table 1 (the complete list of identified peptides is available in Supporting Information S2). The developed mGCB@TiO_2 stationary phase could enrich up to 32 phosphopeptides, with an enrichment ratio of 22%.

Table 1. Total identified peptides and phosphopeptides for each experimental replicate (R1, R2) in the preliminary experiments, with related enrichment.

mGCB@TiO_2	Total peptides	Casein phosphopeptides	E (%)[a]
HNO_3-treated R1	145	32	22%
HNO_3-treated R2	130	29	22%
No HNO_3 R1	146	12	8%
No HNO_3 R2	151	16	10%
HNO_3-treated R1[b]	132	30	23%
HNO_3-treated R2[b]	134	30	22%

[a] Enrichment (%) = [phosphopeptides/total peptides x 100]

[b] one month later

All types of carbon blacks expose on their surface several functional groups due to oxygen chemisorption. These groups are oxygen complexes, having a structure similar to hydroquinone, quinones, chromene and benzpyrylium salts. These groups are able to interact so strongly with sufficiently acidic compounds that conventional solvent systems are not able to desorb them.[33] Therefore, GCB has a somewhat positively charged surface that also sorbs by an anion-exchange mechanism. The types of interactions comprise hydrophobic, electronic and ion-exchange with analytes. Because of the presence of positively charged chemical heterogeneities on the surface, GCB can be considered to be both reversed-phase (RP) sorbent and anion exchanger. Additionally, GCB can be employed to separate neutral from basic compounds from acidic ones.[34] Therefore, GCB exhibits the advantage of high affinity for organic acidic compounds, and could be suitable for the separation of phosphopeptides. For this reason, preliminary experiments were performed in order to avoid oxidation of the starting GCB. The material was not treated with HNO_3 but directly autoclaved to deposit magnetite and TiO_2. The product could be obtained and still retained magnetic properties, thus we employed it for enrichment from the standard tryptic mixture of BSA and casein, as already done for the normal material. Results are reported in Table 1; despite the good mechanical performance of the non-oxidized composite, the recovery was not comparable to the oxidized one, and the overall binding capacity was seriously compromised as well as the selectivity to the target phosphopeptides. Thus, only the oxidized GCB was further employed for tests.

The efficiency of the material was finally tested over time. In fact, materials for enrichment may degrade over time and their selectivity can be significantly reduced. In the case of the present composite this was not observed at all, and the enrichment capacity on the BSA:casein mixture, 100:1, was comparable a month later after preparation (Table 1). Thus the material was prepared twice: the first batch was employed for comparative study and method optimization, whereas the second one was employed to test the effect of batch preparation on the enrichment process.

Method optimization on yeast extracts.

After the preliminary positive results on the BSA:casein, 100:1 sample, the developed composite was tested on a real cell extract. In most of the works in which new phases are proposed for application to phosphopeptide enrichment the developed materials are tested on simulated mixtures, as the BSA:casein mixture described in the previous paragraph, but results were monitored mainly by MALDI MS, directly without any separation. This approach is suitable for relatively simple samples as is the case of a standard peptide mixture, but it is not applicable to a real sample, where separation is necessary. The important point is that direct detection cannot be applied to real complex samples, such as cell extracts, which are the final matrices to which such systems will be applied, if sufficient performance is achieved relative to available systems. The integration of the enrichment protocol into a shotgun proteomics workflow would allow for better comparison with other systems and better evaluation of the actual potential of the newly developed phase. For this reason, we decided to apply the composite to a yeast extract for phosphopeptide enrichment and comparison to commercial TiO_2 spin columns. Yeast was preferred over standard cell lines because it is cheap, readily commercially available and it does not need any specific biological equipment for production, as opposed to the case of cell lines. At the same time, yeast is a complex matrix for which up to 3477 phosphoproteins were identified.[35] This makes yeast extracts a convenient matrix to better test the enrichment efficiency of new materials for phosphoproteomics applications.

One important factor potentially affecting the selectivity of phosphopeptide enrichment is the ratio of stationary phase amount to protein digest quantity.[36] It was demonstrated for TiO_2 beads that the trend of enrichment efficiency was strongly dependent on the ratio between loaded sample and stationary phase, following a Gaussian distribution where enrichment was strongly reduced in presence of an excess or lack of stationary phase. We expected the same trend also for the new mGCB@TiO_2 composite, as well as a dependence on the type of sample being employed, thus different ratios were tested to improve the number of identified phosphopeptides from yeast. The preliminary experiments on the BSA:casein mixture were performed employing 5 mg of the mGCB@TiO_2 stationary phase, thus the same amount was also initially employed for enrichment from yeast extracts. In these conditions up to 2150 phoshopeptides were detected, out of more than 11000 total peptide identifications, with a moderate enrichment of 19% (Table 2). However, the developed material has a large surface area, so an improvement with smaller amounts of stationary phase could be expected in order to avoid saturation of the phase itself. Thus, the optimization of this feature was performed employing the starting 5 mg phase, as in preliminary experiments, and comparing results to 2 mg and 1 mg experiments (Table 2).

Table 2. Total identified peptides and phosphopeptides for each experimental replicate (R1, R2) in the different conditions, with related enrichment.

	Exp. replicate	Total peptides	Total phosphopeptides	E (%)[a]
5 mg mGCB@TiO_2	R1	11125	2150	19%
	R2	11179	2016	18%
2 mg mGCB@TiO_2	R1	7940	3408	43%
	R2	8881	3212	48%
1 mg mGCB@TiO_2	R1	7719	3011	39%
	R2	6710	3034	34%
Commercial spin column	R1	8332	3210	38%
	R2	8709	3102	36%
2 mg mGCB@TiO_2 (2nd batch)	R1	7353	2988	41%
	R2	6279	2767	44%

[a] Enrichment (%) = [phosphopeptides/total peptides x 100]

The results are reported for the two experimental replicates combining data from three technical replicates. As expected, the reduction of mGCB@TiO_2 amount improved the number of identified phosphopeptides from yeast extract, passing from 2150 and

2016 phosphopeptides for 5 mg to 3408 and 3212 phosphopeptides for 2 mg experiments. The increase was particularly significant when considering the enrichment (Table 2). In fact, reducing the stationary phase amount from 5 mg to 2 mg had more than doubled the enrichment efficiency, from 18% and 19% of 5 mg experiments up to 43% and 48% for 2 mg experiments.

The further reduction of mGCB@TiO_2 amount from 2 mg to 1 mg did not provide a similar improvement. In fact, the total number of recovered phosphopeptides decreased to 3011 and 3034 total phosphopeptide for the two replicates. Additionally, the enrichment was also affected and decreased to 39% and 34%. Therefore, the best conditions were obtained with 2 mg amounts.

This result was compared to the one obtained with the commercial TiO_2 spin column, with equivalent experimental conditions: despite both systems employ TiO_2 to selectively capture phosphopeptides, the results obtained by enriching 300 µg of tryptic yeast digest on both phases were different. In particular, with the optimized protocol the mGCB@TiO_2 enrichment was more efficient, and allowed to detect up to 3408 and 3212 phosphopeptides, compared to 3210 and 3102 of the commercial TiO_2 spin column. Not only were the absolute numbers better for the developed system, but also the enrichment efficiency, which could reach up to 48% against 38% as the best result of the commercial spin columns. Therefore, both the total number of phosphopeptides identified and the selectivity were better for the developed system.

The results provided by both experimental replicates were employed to further compare results between the different tested conditions. If non-redundant phospho-sequences (regardless of phospho-isomers) were considered, then the distribution across experiments is reported in Figure 2a.

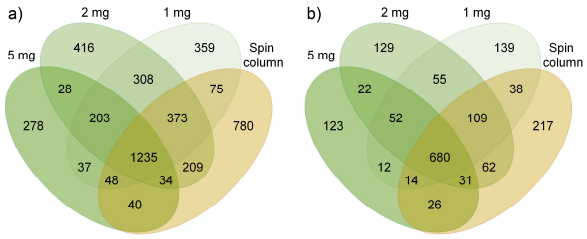

Figure 2. Venn diagrams reporting the distribution of: a) non-redundant phospho-sequences (regardless of phospho-isomers) and b) phosphoproteins, across the different mGCB@TiO_2 experimental conditions and for TiO_2 commercial spin column.

The largest number of unique phospho-sequences was detected with the mGCB@TiO_2 material, 2 mg experiment, which provided 2806 unique phospho-sequences (63% of all identified unique phospho-sequences). The commercial spin column performed similarly, with 2794 unique phospho-sequences (63%), whereas the 1 mg and 5 mg experiments gave lower numbers, with a total of 2638 (60%) and 1903 (43%) sequences, respectively. Most sequences (28%) were shared across all conditions. The contribution of 5 mg and 1 mg experiments which was not detected in the 2 mg experiments was low, 18% of the total, while a partial complementarity was observed with the commercial TiO_2 spin column: 41% of the sequences were common to both mGCB@TiO_2 (2 mg experiments) and the commercial spin column, while 21% of the sequences were individually provided by both enrichment systems.

If a similar analysis was performed taking into consideration the identified phosphoprotein groups in the different conditions, the situation was similar (Figure 2b). Among the tested conditions for mGCB@TiO_2, the best results were confirmed for the 2 mg experiments, which provided for the two combined experimental replicates a total of 1140 phosphoproteins. The 5 mg experiments provided the least number, with a total of 960 phosphoproteins, whereas a further reduction to 1 mg basically did not provide an improvement but results comparable to the 2 mg experiments, with 1099 identified phosphoproteins. The same consideration for the commercial TiO_2 spin column gave similar numbers to the 2 mg mGCB@TiO_2 results, providing 1177 phosphoproteins. Most of them, 40% of the total phosphoprotein identifications, were shared across all the experiments, whereas the unique contribution was small.

Thus, the results pointed out that the new composite mGCB@TiO_2 and the commercial spin column performed similarly; finally, we considered the number of phosphopeptides vs the Log2 raw intensity bins (Figure 3) to compare the intensity of the identified phosphopeptides between the 2 mg mGCB@TiO_2 experiments and the TiO_2 spin column results. Such consideration showed some difference could be appreciated at this level, and the intensity was twice more intense for the mGCB@TiO_2 composite, relative to the commercial spin column. This could be a beneficial feature for detecting lower abundant peptides and for label-free quantification of phosphopeptides.

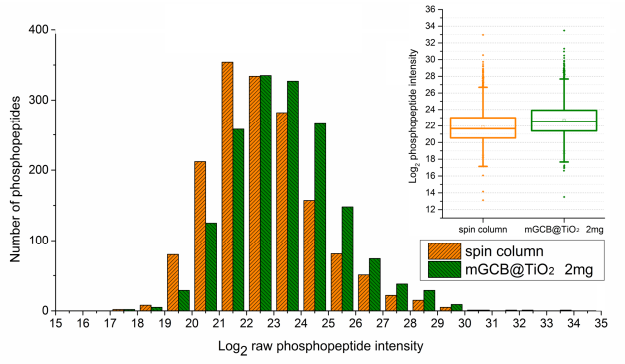

Figure 3. Number of phosphopeptides vs the Log2 raw intensity bins for mGCB@TiO_2 (2 mg experiment) and TiO_2 commercial spin column.

Finally, the physico-chemical features of the isolated peptides were considered. The GRAVY (grand average of hydropathy) values and the pI of the peptides isolated by mGCB@TiO_2 and the commercial spin columns were calculated and compared, dividing the peptides into two groups, the isolated phosphopeptides and the co-isolated non-phosphopeptides. By such comparison it was possible to observe that the GRAVY values and pI of the isolated phosphopeptides did not significantly differ between the two groups, as a result that the mechanisms at the basis of phosphopeptides isolation is driven by the affinity to TiO_2 and is not affected by the presence of mGCB beneath it. The same applied to the pI of non-phosphopeptides, however some significant differences were observed for their GRAVY values (Figure 4).In fact, in the case of the commercial TiO_2 spin columns, a larger percentage of co-enriched peptides had an hydrophobic character, with 36% of them having a GRAVY value $0 < x \leq 1$. However, for the same GRAVY value interval, the percentage is only 12 for the developed mGCB@TiO_2 composite, which also co-enriched a larger amount of more hydrophilic peptides, with 34% of them having a GRAVY ≤ -1 vs only 13% for the same interval for the commercial spin column. This consideration, together with recent findings supporting that a hydrophilic phase would improve enrichment by reducing unspecific binding,[28,37,38] could be accounted for the better selectivity of the composite than pure TiO_2.

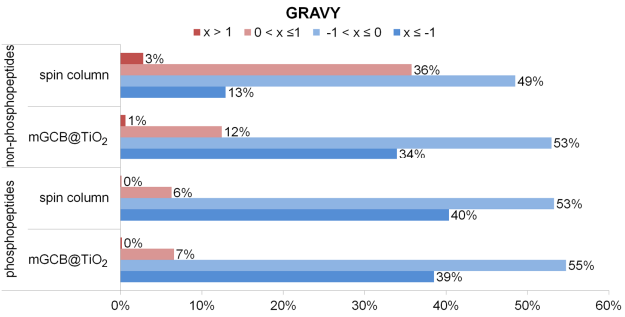

Figure 4. Graph summarizing the GRAVY value distribution of identified phosphopeptide and non-phosphopeptides for the mGCB@TiO_2 composite and the commercial TiO_2 spin column.

At the end of the comparison we evaluated the reproducibility of mGCB@TiO_2 production. A new batch was prepared and employed with the optimized conditions (Table 2). These experiments provided 2988 and 2767 total phosphopeptides, which were lower in number than the results of previous experiments. However the enrichment efficiency was always above 40%, with 41% and 44% for the two replicates. The lower number of total identifications should not be misleading, as the large variability was due to the sample itself. Commercial yeast paste is no standard; therefore, variations could be observed. However, it is readily available and provides a more complex system than the ones usually employed at development level, mainly casein and BSA mixtures, which are good for proof of principle only.

■ CONCLUSION

In the described experiments a new material was produced, employing GCB as support for TiO_2. GCB was previously magnetized to allow for better enrichment and concentration of target phosphopeptides. In this sense an oxidizing step was necessary for the purpose of enrichment, as pointed out by preliminary experiments. The extensive physico-chemical characterization of the final material and intermediate products confirmed the successful production of the desired composite and the preservation of the gra-

phitic structure. However, the functionalization with Fe_3O_4 first and TiO_2 as the final step greatly reduced the large surface area of pristine GCB. Nevertheless, the prepared composite could efficiently enrich phosphopeptides, both from a simulated complex mixture of BSA and casein tryptic digests, and from a real yeast extract. In this regard we chose to optimize and test the new composite within a typical shotgun proteomics workflow, which is the one suitable for application to real large-scale phosphoproteomics experiments and, most importantly, which would really enable to assess differences between the new system and established ones. After optimization of the composite amount employed for 300 µg experiments, a final comparison to commercial TiO_2 spin columns was performed, with better results, which provided up to 3408 and 48% enrichment for mGCB@TiO_2, vs 3210 and 38% enrichment for the commercial kit. Reproducible results were obtained with a new batch of mGCB@TiO_2 and new yeast extract. Therefore, a new composite based on GCB was developed for the first time, which provided better results than the commercial device. Apart from this, the work points out how it is important to test and evaluate the new materials for phosphoproteomics on real workflows, because in this way differences which could not be visible at the simulated mixture level or with approaches other than shotgun proteomics can be really appreciated and would help in filling the gap for existing phosphopeptide enrichment strategies.

ASSOCIATED CONTENT

Supporting Information

The Supporting Information is available free of charge on the ACS Publications website.

Supporting Information S1 contains the TEM and porosimetry data for GCB materials.
Supporting Information S2 (Excel) contains the list of the identified peptides in the preliminary experiments with BSA:casein, 100:1.
Supporting Information S3 (Excel) contains the list of the identified peptides in tin yeast experiments.

AUTHOR INFORMATION

Corresponding Author

* E-mail: aldo.lagana@uniroma1.it

Author Contributions

The manuscript was written through contributions of all authors. All authors have given approval to the final version of the manuscript.

Notes

The authors declare no competing financial interest.

ACKNOWLEDGMENT

The authors wish to thank Dr. Pettiti for porosimetry measurements.

REFERENCES

(1) Lampe, P. D.; Lau, A. F. *Int. J. Biochem. Cell Biol.* **2004**, *36*, 1171–1186.
(2) Gahmberg, C. G.; Fagerholm, S. C.; Nurmi, S. M.; Chavakis, T.; Marchesan, S.; Grönholm, M. *Biochim. Biophys. Acta - Gen. Subj.* **2009**, *1790*, 431–444.
(3) Mayr, B.; Montminy, M. *Nat. Rev. Mol. Cell Biol.* **2001**, *2*, 599–609.
(4) O'Connor, D. S.; Grossman, D.; Plescia, J.; Li, F.; Zhang, H.; Villa, A; Tognin, S.; Marchisio, P. C.; Altieri, D. C. *Proc. Natl. Acad. Sci. U. S. A.* **2000**, *97*, 13103–13107.
(5) Cohen, P. *Nat. Rev. Drug Discov.* **2002**, *1*, 309–315.
(6) Ruprecht, B.; Lemeer, S. *Expert Rev. Proteomics* **2014**, *11*, 259–267.
(7) Li, X.-S.; Yuan, B.-F.; Feng, Y.-Q. *TrAC Trends Anal. Chem.* **2016**, *78*, 70–83.
(8) Blacken, G. R.; Sadílek, M.; Tureček, F. *J. Mass Spectrom.* **2008**, *43*, 1072–1080.
(9) Zhou, H.; Ye, M.; Dong, J.; Corradini, E.; Cristobal, A.; Heck, A. J. R.; Zou, H.; Mohammed, S. *Nat. Protoc.* **2013**, *8*, 461–480.
(10) Feng, S.; Ye, M.; Zhou, H.; Jiang, X.; Jiang, X.; Zou, H.; Gong, B. *Mol. Cell. Proteomics* **2007**, *6*, 1656–1665.
(11) Yu, L. R.; Veenstra, T. In *Methods in molecular biology (Clifton, N.J.)*; Humana Press: New York, 2013; Vol. 1002, pp 93–103.
(12) Nelson, C. A.; Szczech, J. R.; Xu, Q.; Lawrence, M. J.; Jin, S.; Ge, Y. *Chem. Commun.* **2009**, 6607–6609.
(13) Engholm-Keller, K.; Larsen, M. R. In *Phospho-Proteomics*; Stechow, L. von, Ed.; Springer New York: New York, 2016; pp 161–177.
(14) Wakabayashi, M.; Kyono, Y.; Sugiyama, N.; Ishihama, Y. *Anal. Chem.* **2015**, *87*, 10213–10221.
(15) Ruprecht, B.; Koch, H.; Medard, G.; Mundt, M.; Kuster, B.; Lemeer, S. *Mol. Cell. Proteomics* **2015**, *14*, 205–215.
(16) Li, X.-S.; Zhu, G.-T.; Luo, Y.-B.; Yuan, B.-F.; Feng, Y.-Q. *TrAC - Trends Anal. Chem.* **2013**, *45*, 233–247.
(17) Ai Ling Tang, L.; Wang, J.; Kwang Lim, T.; Bi, X.; Cheng Lee, W.; Lin, Q.; Chang, Y.-T.; Teck Lim, C.; Ping Loh, K. *Anal. Chem.* **2012**, *84*, 6693–9700.

(18) Cheng, G.; Yu, X.; Zhou, M. M.-D.; Zheng, S. S.-Y. *J. Mater. Chem. B* **2014**, *2*, 4711.
(19) Lu, J.; Deng, C.; Zhang, X.; Yang, P. *ACS Appl. Mater. Interfaces* **2013**, *5*, 7330–7334.
(20) Capriotti, A. L.; Cavaliere, C.; Foglia, P.; Samperi, R.; Stampachiacchiere, S.; Ventura, S.; Lagan??, A. *Anal. Bioanal. Chem.* **2015**, *407*, 1706–1719.
(21) Cavaliere, C.; Capriotti, A. L.; Foglia, P.; Piovesana, S.; Samperi, R.; Ventura, S.; Laganà, A. *J. Sep. Sci.* **2015**, *38*, 3599–3606.
(22) Wang, Z.-G.; Lv, N.; Bi, W.-Z.; Zhang, J.-L.; Ni, J.-Z. *ACS Appl. Mater. Interfaces* **2015**, *7*, 8377–8392.
(23) Jersie-Christensen, R. R.; Sultan, A.; Olsen, J. V. 2016; pp 251–260.
(24) Zhai, R.; Tian, F.; Xue, R.; Jiao, F.; Hao, F.; Zhang, Y.; Qian, X. *RSC Adv.* **2016**, *6*, 1670–1677.
(25) Yang, H.; Deng, C.; Zhang, X. *Talanta* **2016**, *153*, 285–294.
(26) Huang, X.; Wang, J. P.; Liu, C. C.; Guo, T.; Wang, S. *J. Mater. Chem. B* **2015**, *3*, 2505–2515.
(27) Zhou, H.; Ye, M.; Dong, J.; Corradini, E.; Cristobal, A.; Heck, A. J. R.; Zou, H.; Mohammed, S. *Nat. Protoc.* **2013**, *8*, 461–480.
(28) Piovesana, S.; Capriotti, A. L.; Cavaliere, C.; Ferraris, F.; Samperi, R.; Ventura, S.; Laganà, A. *Anal. Chim. Acta* **2016**, *909*, 67–74.
(29) Yan, Y.; Zheng, Z.; Deng, C.; Zhang, X.; Yang, P. *Talanta* **2014**, *118*, 14–20.
(30) Ma, M.; Zhang, Y.; Yu, W.; Shen, H. Y.; Zhang, H. Q.; Gu, N. *Colloids Surfaces A Physicochem. Eng. Asp.* **2003**, *212*, 219–226.
(31) Moya, A.; Cherevan, A.; Marchesan, S.; Gebhardt, P.; Prato, M.; Eder, D.; Vilatela, J. J. *Appl. Catal. B Environ.* **2015**, *179*, 574–582.
(32) Jabeen, F.; Najam-Ul-Haq, M.; Rainer, M.; Güzel, Y.; Huck, C. W.; Bonn, G. K. *Anal. Chem.* **2015**, *87*, 4726–4732.
(33) Hennion, M. C. *J. Chromatogr. A* **2000**, *885*, 73–95.
(34) Hennion, M. C. *J. Chromatogr. A* **1999**, *856*, 3–54.
(35) Yachie, N.; Saito, R.; Sugiyama, N.; Tomita, M.; Ishihama, Y. *PLoS Comput. Biol.* **2011**, *7*, e1001064.
(36) Li, Q. R.; Ning, Z. Bin; Tang, J. S.; Nie, S.; Zeng, R. *J. Proteome Res.* **2009**, *8*, 5375–5381.
(37) Novotna, L.; Emmerova, T.; Horak, D.; Kucerova, Z.; Ticha, M. *J. Chromatogr. A* **2010**, *1217*, 8032–8040.
(38) Zhang, L.; Zhao, Q.; Liang, Z.; Yang, K.; Sun, L.; Zhang, L.; Zhang, Y. *Chem. Commun.* **2012**, *48*, 6274–6276.

Authors are required to submit a graphic entry for the Table of Contents (TOC) that, in conjunction with the manuscript title, should give the reader a representative idea of one of the following: A key structure, reaction, equation, concept, or theorem, etc., that is discussed in the manuscript. Consult the journal's Instructions for Authors for TOC graphic specifications.